Investigating the salinity effect on water retention property and microstructure changes along water retention curves for lime-treated soil

Zi Ying[1], Yu-Jun Cui[1], Nadia Benahmed[2], Myriam Duc[3]

[1]: Ecole des Ponts ParisTech, Laboratoire Navier/CERMES, 6-8 av. Blaise Pascal, Cité Descartes, Champs-sur-Marne, 77455 Marne-la-Vallée cedex 2, France

[2]: INRAE, Aix Marseille Univ, RECOVER, Equipe G2DR, 3275 route Cézanne, CS 40061, 13182 Aix-en-Provence, France

[3]: Université Gustave Eiffel/GERS/SRO, 14-20 boulevard Newton, Champs-sur-Marne, 77447 Marne-la-Vallée, France

Corresponding author:

Dr. Zi YING

Ecole des Ponts ParisTech, Laboratoire Navier/CERMES
6-8 av. Blaise Pascal, Cité Descartes, Champs-sur-Marne

77455 Marne-la-Vallée Cedex 2, France

E-mail: zi.ying@enpc.fr

Abstract:

Lime treatment is a widely applied technique in improving the workability and geotechnical properties of soil. The water retention property and microstructure are highly related to the hydro-mechanical behaviour of unsaturated lime-treated soil. In this study, the water retention property and the evolution of pore size distribution (PSD) along the water retention curves (during drying) were studied for a lime-treated soil, with emphasis put on the curing time and salinity effects. Two soil powders with different soil salinities were prepared and stabilised by 2% lime. The chilled-mirror dew-point hygrometer and the contact filter paper method were used to measure the total and matric suctions, respectively. The PSD of lime-treated soil at various water contents was obtained using mercury intrusion porosimetry (MIP). Results showed that the matric suction increased significantly, while the total suction varied slightly during curing. At a given curing time, the specimens with higher salinity exhibited higher matric and total suctions. The difference between the soil water retention curves (SWRCs) determined by the filter paper method and from the PSD became more significant at longer curing time, as the production of cementitious compounds did not contribute to the SWRC from PSD, but contributed to the increase of matric suction measured by the filter paper method. The PSD of lime-treated soil changed from bi-modal characteristics ($w > 14\%$) to tri-modal pattern ($w \approx 8\%$), and finally recovered to bi-modal characteristics ($w \approx 3\%$), due to the shrinkage-related cracking of the clay fraction. The lime treatment inhibited the clay shrinkage, whereas the curing time and salinity effects on the drying-induced microstructure were insignificant.

Keywords: lime-treated soil; salinity; total suction; matric suction; microstructure

1. Introduction

From a socio-economic point of view, there is an increasing need of using local soils in geotechnical and geo-environmental constructions such as embankments, dikes, slopes and municipal waste barriers. However, when the natural soils involved have low physical and mechanical properties and cannot be directly used in the constructions, lime treatment is often applied to improve the workability and the mechanical properties of soils through a series of physical-chemical reactions, including lime hydration, cation exchanges and long-term pozzolanic reaction [1-3].

The water retention property describing the relationship between suction and either water content or degree of saturation was widely used to predict the permeability [4,5], shear strength [6], deformation [7] for unsaturated soils. It is also an important factor affecting the hydro-mechanical behaviour of lime-treated soils. In general, the lime addition first resulted in the flocculation of soil particles, forming coarser aggregates with larger macro-pores [8]. During curing, the cementitious compounds produced from the pozzolanic reaction coated the surface of aggregates and filled some pores, leading to the reduction of pore size and interconnectivity [9–13], giving rise to higher water retention property and mechanical performance of lime-treated soil. The production of cementitious compounds was affected by the existence of salts in soil. Ramesh et al. [14] reported that the sodium salts in fly ash-lime mixtures could promote the formation of sodium calcium silicate hydrate as compared to calcium silicate hydrate. Saldanha et al. [15] found that 1% NaCl was the optimum salt content in lime-treated soil, while a higher concentration would decrease the rate of lime dissociation. Nevertheless, Xing et al. [16] indicated that the Al^{3+} and Ca^{2+} ions in cemented salt-rich soil improved the formation of cementitious compounds, while the Mg^{2+}, Cl^{-} and SO_4^{2-} ions impeded such formation.

The soil water retention curves (SWRCs) can be determined experimentally by the chilled-mirror dew-point hygrometer [17] and non-contact filter paper method [18,19] for the total suction measurement, as well as by contact filter paper method [19], insertion tensiometer [20] and axis-translation technique [21,22] for the matric suction measurement. The SWRCs in terms of matric suction can be also derived from the pore size distribution (PSD) curves obtained from mercury intrusion porosimetry (MIP) test [5]. However, some difference between the SWRCs from direct measurements and from MIP tests was often observed. This difference was mainly attributed to the volume change due to suction changes, because the SWRC determined directly involved the effect of volume change, while the SWRC derived from MIP

test did not [9,23,24].

In most cases, the lime-treated soils are exposed to natural environment and unavoidably subjected to water evaporation effect. Drying can generate soil shrinkage and desiccation cracks, which might have a detrimental effect on the sustainability of infrastructures. For the compacted untreated soil, under the effect of drying, the frequency and modal size of macro-pores decreased while the frequency of micro-pores increased, due to the clay shrinkage that transformed some macro-pores to micro-pores [25–29]. Stoltz et al. [30] found that the lime treatment did not prevent the soil shrinkage. However, Nabil et al. [31] and Poncelet and François [32] indicated that the lime treatment would reduce the shrinkage potential and attenuated the propagation of desiccation macro-cracks of silty clay, due to the formation of cementitious compounds limiting the development of cracks.

It appears from the aforementioned studies that although the water retention property and desiccation cracks of lime-treated soils were investigated, few attention has been paid to the salinity effect on the water retention property during curing and to the changes of microstructure along the water retention curve (during drying) for lime-treated soil. However, while dealing with constructions involving salted soils, the salinity effect becomes an essential parameter for the assessment of the effectiveness of lime treatment. This constitutes the main objective of this study. In this paper, the chilled-mirror dew-point hygrometer (WP4C) and the contact filter paper (FP) method were employed to determine the SWRCs of lime-treated soil with different salinities. The evolution of PSD along SWRC was investigated by MIP tests. The SWRCs were also derived from PSD curves, for the purpose of comparison with the direct measured ones. The results obtained revealed the different evolution of matric suction and total suction with curing time, and the effect of microstructure changes on SWRC during drying, for lime-treated soil with different salinities.

2. Materials and methods

2.1 Materials

The soil used was a plastic silt, taken from Les Salins de Giraud in southern France, which was used for a dike construction. This natural soil (w = 15.6%) was saline with soil salinity of 2.1‰ (g of salt/kg of dry soil) and water salinity of 13.3‰ (g of salt/kg of salty water) [33]. The geotechnical properties are presented in Table 1. As shown in Fig. 1, this soil contains 17%

clay-size particles, 53% silt and 30% fine sand. X-Ray diffraction (XRD) analysis shows that the soil is composed of 15.7% clay minerals and 84.3% non-clay minerals. The non-clay minerals are identified as 39% quartz, 35% calcite, 9.5% feldspar and 0.8% halite NaCl, and the clay minerals consists of 10.8% illite, 3.6% chlorite and 1.3% kaolinite. The main ion species in soil pore water are Cl^-, Na^+, K^+, Ca^{2+}, and Mg^{2+}, which are similar to the salt composition of synthetic seawater. Thus, to prepare the salted soil, five different salts of synthetic seawater were used according to the French standard [34], as shown in Table 2. The target soil salinity of salted soil was selected as 6.8‰ (g of salt/kg of dry soil) which corresponded to the water salinity of 34‰ (g of salt/kg of salty water) for soil at 20% water content. This water salinity was exactly the salinity of synthetic seawater. More details about the salted soil preparation can be found in Ying et al. [33]. The natural saline soil (r' = 2.1‰) and salted soil (6.8‰) were air-dried, ground and passed through 0.4 mm sieve.

Table 1. Characteristics of the tested soil.

Property	Value
Liquid limit, w_L (%)	29
Plastic limit, w_p (%)	19
Plasticity Index, I_p	10
Specific gravity, *Gs*	2.71
Specific surface area (m^2/g)	24

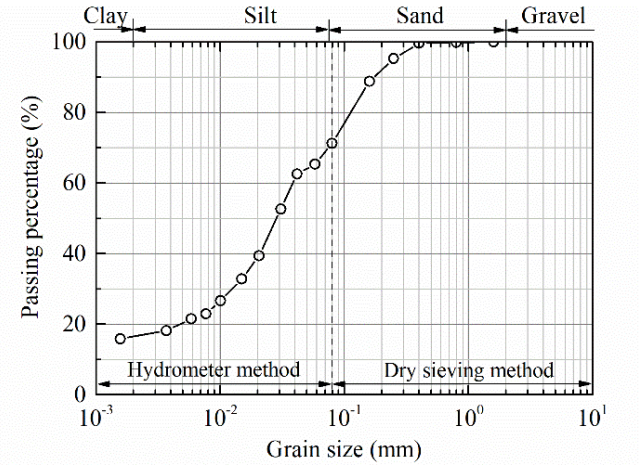


Fig. 1. Grain size distribution of the tested soil.

Table 2. Salt composition of synthetic seawater.

Salts	NaCl	$MgCl_2 \cdot 6H_2O$	$MgSO_4 \cdot 7H_2O$	$CaSO_4 \cdot 2H_2O$	$KHCO_3$
Concentration (g/L)	30.0	6.0	5.0	1.5	0.2

A quicklime with CaO content as high as 97.3% was used as additive. Based on the dosage applied for the construction of dike at Les Salins de Giraud, a lime content of 2% by weight of dry soil was selected.

To prepare the soil specimen, the dry soil powder was first mixed with lime and then humidified by deionized water to obtain the target water content (w = 17%). According to the proctor compaction curve of lime-treated natural soil with soil salinity of 2.1‰ (Fig. 2), all the specimens with different soil salinities were statically compacted to the same dry density (1.63Mg/m^3). A compaction rate of 0.3 mm/min was adopted. After compaction, the specimens were wrapped by plastic film and scotch tape, covered by wax, confined in a hermetic box and cured for different times.

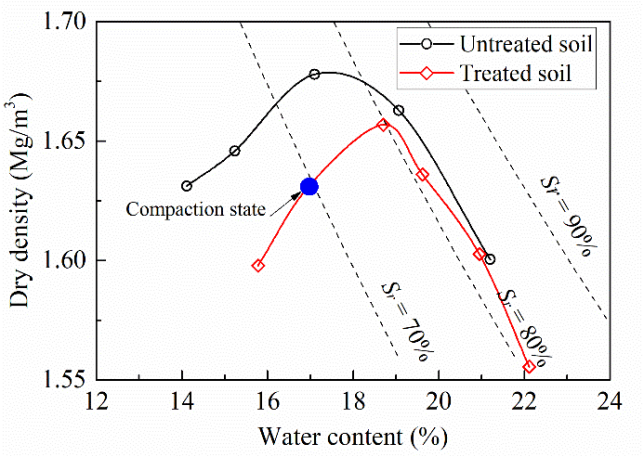


Fig. 2. Proctor compaction curves of untreated and lime-treated soils with soil salinity of 2.1‰.

2.2 Test methods

The soil total suction was determined by WP4C device [17]. The specimen (38 mm in diameter and 100 mm in height) was cut into several small pieces at given curing time. Each small piece was air-dried for different durations to reach different water contents. Then, they were covered and stored for one night for water homogenization. Afterwards, one small piece was put into the WP4C device for total suction measurement. Immediately after suction measurement, the

small piece was oven-dried to determine the water content.

Matric suction was measured using contact filter paper method [19]. At given curing time, the lime-treated specimens (50 mm in diameter and 20 mm in height) were air-dried for different times to reach different target water contents, in order to obtain the soil specimens with different matric suctions. During drying, the water contents of specimens were controlled by weighing the masses of specimens. Once the target water content reached, the three stacked filter papers were sandwiched between two specimens with the same water content for one matric suction measurement. Two replicated tests were conducted and the mean value was used.

After matric suction measurement, one specimen was directly oven-dried to determine its water content, while the second one was cut into small pieces for the MIP test. The small pieces were rapidly frozen using vacuumed liquid nitrogen, and lyophilised following the procedure proposed by Delage and Lefebvre [35]. Then they were subjected to MIP test.

In the MIP test, the entrance pore diameter can be deduced from the mercury intrusion pressure according to Laplace's law and a relationship between mercury and water can be established:

$$d = -\frac{4T_m \cos\theta_m}{p_m} = \frac{4T_w \cos\theta_w}{p_w} \tag{1}$$

where subscript m denotes mercury while subscript w denotes water; T is the surface tension (T_w = 0.073 N/m, T_m = 0.485 N/m); p_m is the mercury intrusion pressure; p_w is the soil matric suction; θ is the contact angle ($\theta_w = 0°$, $\theta_m = 130°$).

The pore size density function can be determined as follows [36]:

$$f(\log r_i) = \frac{dv_i}{d(\log d)} \tag{2}$$

where $f(\log r_i)$ is the frequency of density function; dv_i is the intruded mercury volume at a given incremental intrusion pressure. The intruded mercury volume can be transformed to the intruded void ratio by multiplying the density of soil particles.

The matric suction can be deduced from entrance pore diameter:

$$p_w = \frac{4T_w \cos\theta_w}{d} \tag{3}$$

The corresponding water content of soil specimens can be obtained from MIP results [24,37]:

$$w_{MIP} = (1 - S_{rm})(w_{sat} - w_r) + w_r = \frac{e}{G_S}(1 - \frac{e_{MIP}}{e}) \quad (4)$$

where S_{rm} is the saturation degree of mercury; w_{sat} is the water content at saturation; w_r is the residual water content; e is the global void ratio of compacted specimens; e_{MIP} is the mercury intruded void ratio; G_s is the specific gravity.

Based on the matric suction and water content calculated by Eqs. (3) and (4), the water retention curves can be deduced from the pore size distribution curves.

3. Results

3.1 Water retention property

The SWRCs in terms of total and matric suctions are depicted in Figs. 3a and 3b for lime-treated specimens with soil salinities of 2.1‰ and 6.8‰, respectively. Note that the data of lime-treated specimens with 2.1‰ at curing times of 1-, 28- and 90-day were reported previously in Ying et al. [38]. It appears that the curing time had insignificant effect on the SWRCs of total suction, whereas the SWRCs of matric suction shifted rightwards with the increase of curing time from 28 days to 90 days. This suggested that the effect of curing time on the water retention property of lime-treated saline soil was mainly reflected on the changes in matric suction rather than total suction. The difference between the total and matric suctions can be considered as osmotic suction which was resulted from the dissolved salts in soil pore water [39]. As the total suction varied slightly while the matric suction increased significantly with increasing curing time, the osmotic suction of lime-treated specimens seemed to decrease over curing. With decreasing water content, the SWRCs of matric suction converged gradually to the total suction curves. This was consistent with the results of untreated soil obtained by Sreedeep and Singh [39] and Arifin and Schanz [40].

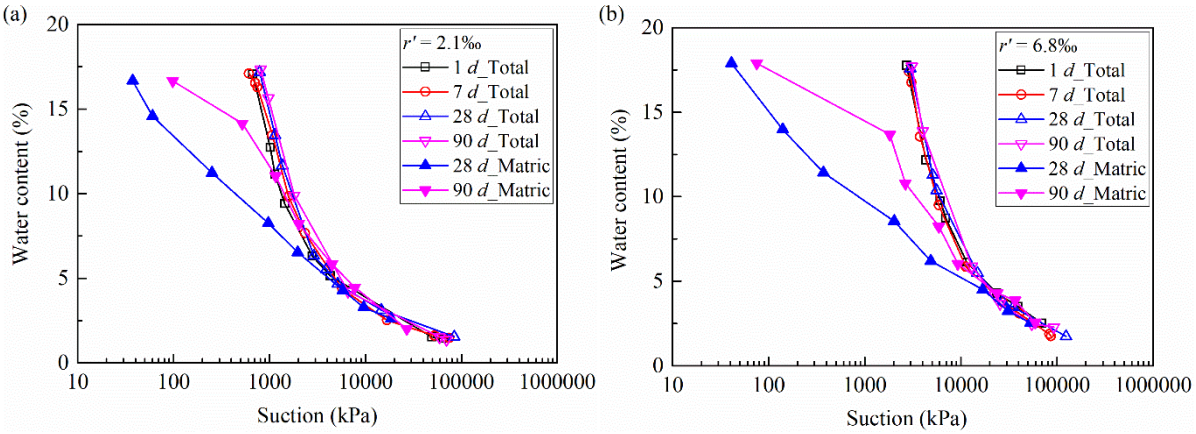


Fig. 3. Water retention curves in terms of total and matric suctions for the lime-treated specimens: (a) r' = 2.1‰; (b) r' = 6.8‰.

The SWRCs of total and matric suctions for the lime-treated specimens with different salinities of 2.1‰ and 6.8‰ are presented in Fig. 4a for the specimens at 28-day curing, and in Fig. 4b for the specimens at 90-day curing. It can be observed that, at a given water content, the total suction increased significantly with increasing soil salinity, which can be attributed to the contribution of higher osmotic suction for the specimens with higher soil salinity (6.8‰ against 2.1‰). The matric suction of lime-treated specimens also increased with increasing soil salinity, which was different from the results of untreated soil that the salinity had negligible effect on the matric suction [41–43].

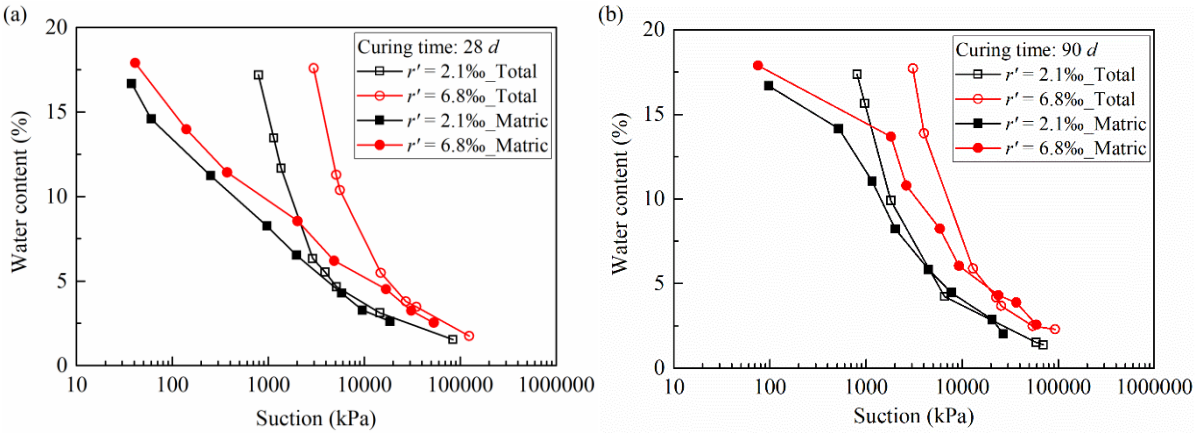
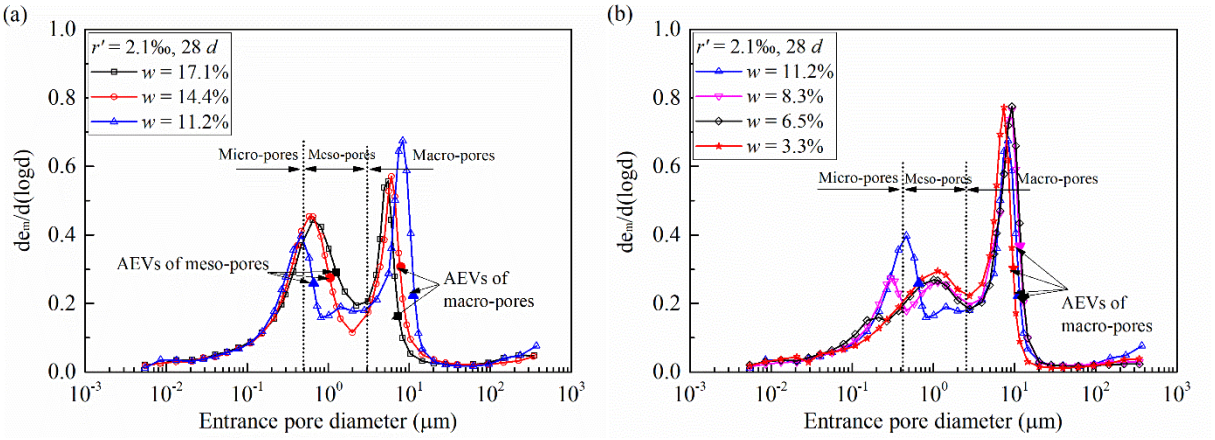


Fig. 4. Salinity effect on the total and matric suctions for the lime-treated specimens: (a) t = 28 days; (b) t = 90 days.

3.2 Microstructure variations along SWRCs

The PSD curves in terms of density function are presented in Figs. 5a and 5b for the specimens cured for 28 days with 2.1‰ soil salinity, and in Figs. 5c and 5d for the specimens at curing

time of 90 days with soil salinities of 2.1‰ and 6.8‰, respectively. Three pore populations of micro-pores, meso-pores and macro-pores can be defined. The boundary between the meso-pores and macro-pores was considered as 3 μm, which was at the minima of PSD curves between two peaks for all the specimens. The delimiting diameter between micro-pores and meso-pores was chosen as 0.5 μm which corresponded to the minima between the two peaks of micro-pores and meso-pores for the specimens at around 8% water content in which the drying-induced micro-pores and meso-pores were well-developed. As shown in Fig. 5a, the as-compacted specimens (w = 17.1%) exhibited bi-modal pore size distribution with two dominant peaks. Upon drying to water content of 14.4% and 11.2%, the peak pore entrance diameter between micro-pores and meso-pores decreased from 0.7 μm to 0.6 and 0.5 μm, while the modal size of macro-pores increased from 5.3 μm to 6.1 μm and 8.2 μm (Fig. 5a). Moreover, an interesting phenomenon was identified from Fig. 5a: a third peak at diameters ranging from 0.9 μm to 3 μm started to appear on the PSD curves of specimens at water content of 11.2%. With drying to 8.3% water content, the two peaks of micro-pores and meso-pores were well developed and the PSD exhibited tri-modal characteristics (Fig. 5b). Upon further drying from 8.3% to 6.5%, the peak frequency ($de_m/d(logd)$) of micro-pores decreased gradually, and the peak of micro-pores disappeared as the specimen was air-dried to 3.3% water content. As shown in Figs. 5c and 5d, the similar evolution trends of PSD during drying were observed for the lime-treated specimens at 90-day curing time with soil salinities of 2.1‰ and 6.8‰: the pore size distribution changed from bi-modal pattern for specimens at higher water content (w > 14%) to tri-modal pattern with drying close to 8% water content; it finally recovered to bi-modal pattern with further drying (w ≈ 3%) as the peak of micro-pores disappeared for both specimens at 90-day curing (r' = 2.1‰ and 6.8‰), in similar manner to the specimens at 28-day curing.



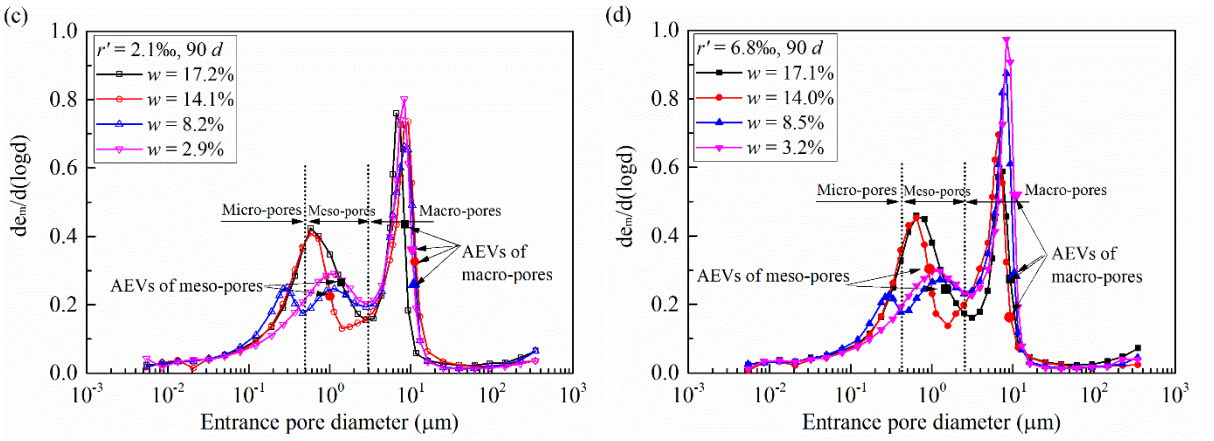


Fig. 5. Pore size distribution of lime-treated specimens during drying: (a) r' = 2.1‰, t = 28 days ($w \geq$ 11.2%); (b) r' = 2.1‰, t = 28 days ($w \leq$ 11.2%); (c) r' = 2.1‰, t = 90 days; (d) r' = 6.8‰, t = 90 days.

Figure 6 shows the variations of void ratio of different pore populations (micro-, meso- and macro-pores) during drying. The global void ratio and water ratio (water volume over solid volume, $e_w = wG_s$, where w is the water content and G_s is the specific gravity) are also presented for comparison. The stacked value of micro-pores, meso-pores and macro-pores represented the total intruded void ratio. For most specimens, the total intruded void ratio coincided well with the global one. Romero et al. [29] and Wan et al. [44] indicated that the smaller pores would be saturated before water began to be stored in the larger pores. Thus, it can be observed that the micro-pores and meso-pores were saturated before drying, as the water ratio was higher than the sum of void ratio of micro-pores and meso-pores at water content of 17% (Fig. 6). During drying, the water ratio decreased gradually, indicating that water withdrew toward the smaller pores. It appears from Fig. 6a that the void ratio of micro-pores increased when the specimens (r' = 2.1‰, t = 28 days) were dried to 11.2% water content, then it decreased with decreasing water content to 3.3%. By contrast, the void ratio of meso-pores decreased, then increased during drying. The void ratio of macro-pores increased with drying to around 8%, then kept almost constant with further drying. As for the specimens (r' = 2.1‰) at 90-day curing (Fig. 6b), the void ratio of micro-pores, meso-pores and macro-pores exhibited similar variations to the specimens at 28-day curing time (Fig. 6a). Concerning the specimens with higher salinity (r' = 6.8‰, t = 90 days), it appears from Fig. 6c that drying had slight effect on the micro-pore void ratio, while it led to a decrease of meso-pore void ratio and an increase of macro-pore void ratio.

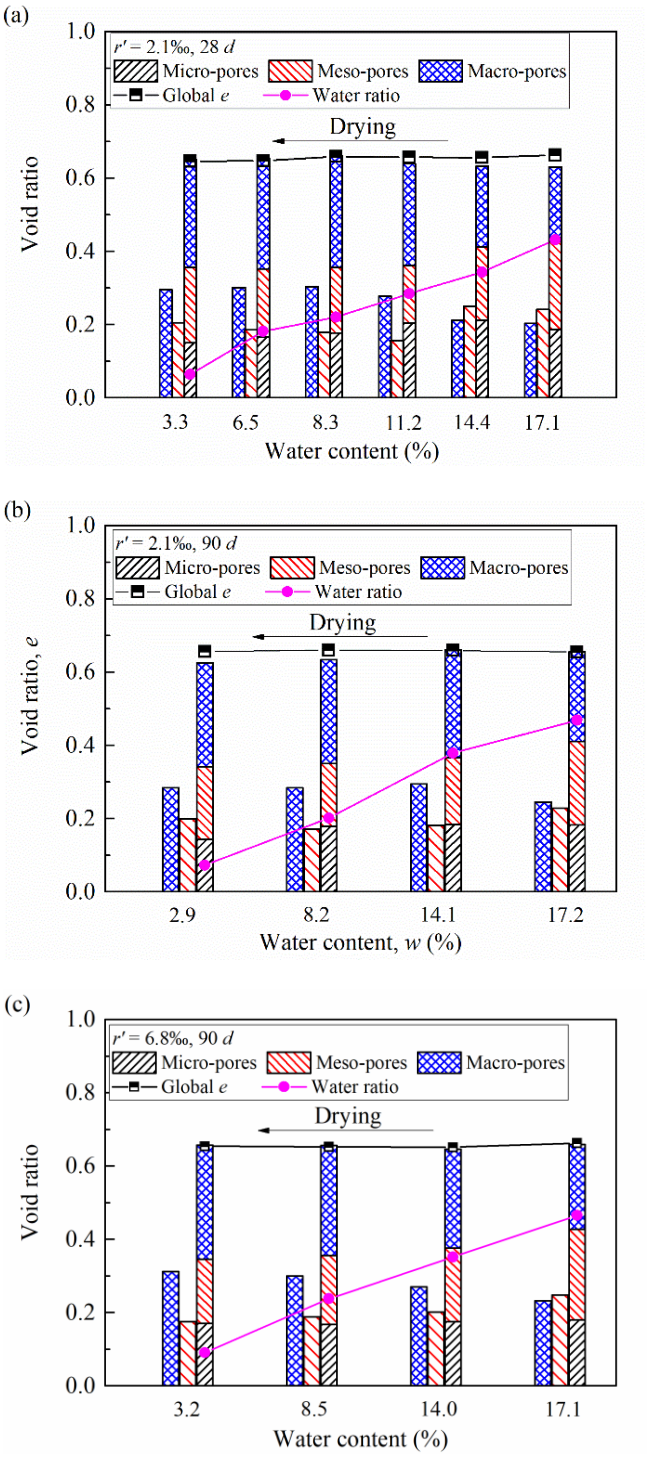


Fig. 6. Variations of void ratio of different pore populations during drying: (a) r' = 2.1‰, t = 28 days; (b) r' = 2.1‰, t = 90 days; (c) r' = 6.8‰, t = 90 days.

The PSD curves of lime-treated soil (r' = 2.1‰) at different curing times are plotted in Figs. 7a and 7b for the specimens at around 8% and 3% water contents respectively. The PSD curves of untreated specimens are also presented for comparison. It appears that, as for the specimens at water content of around 8%, the PSD curves of lime-treated soil at curing times of 28-day and

90-day were almost overlapped, while the curve of untreated soil deviated from that of lime-treated soil. Specifically, the modal sizes of micro-pores and macro-pores were almost identical for untreated and lime-treated specimens, whereas the modal size of meso-pores of lime-treated specimens was smaller than that of untreated specimens. Besides, the lime-treated specimens exhibited a smaller frequency of micro-pores and a higher frequency of macro-pores. As for the specimens at around 3% water content, the PSD curves of lime-treated specimens (t = 28 days and 90 days) exhibited similar modal sizes of meso-pores and macro-pores, while the PSD curves of untreated specimen shifted rightwards slightly, giving rise to larger modal sizes.

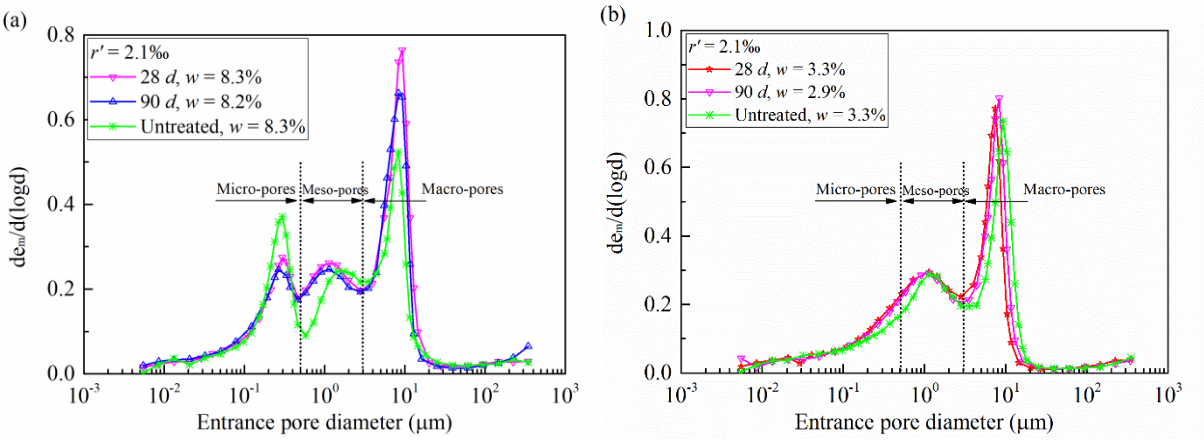


Fig. 7. Lime treatment effect on the pore size distribution of untreated and lime-treated specimens after drying: (a) $w \approx 8\%$; (b) $w \approx 3\%$.

Figure 8 depicts the PSD curves of lime-treated specimens (t = 90 days) with different salinities, but similar water contents ($w \approx 8\%$ in Fig. 8a and $w \approx 3\%$ in Fig. 8b). It can be observed that the salinity effect on the entrance diameter of peak pores was slight, but the salinity had a low but visible effect on the frequencies of peak pores. Specifically, higher frequencies of meso-pores and macro-pores were observed for specimens with higher salinity of 6.8‰ at 8% water content. For specimens at 3% water content, the frequency of meso-pores was rather similar for different salinities, while the frequency of macro-pores was found higher for 6.8‰ soil salinity.

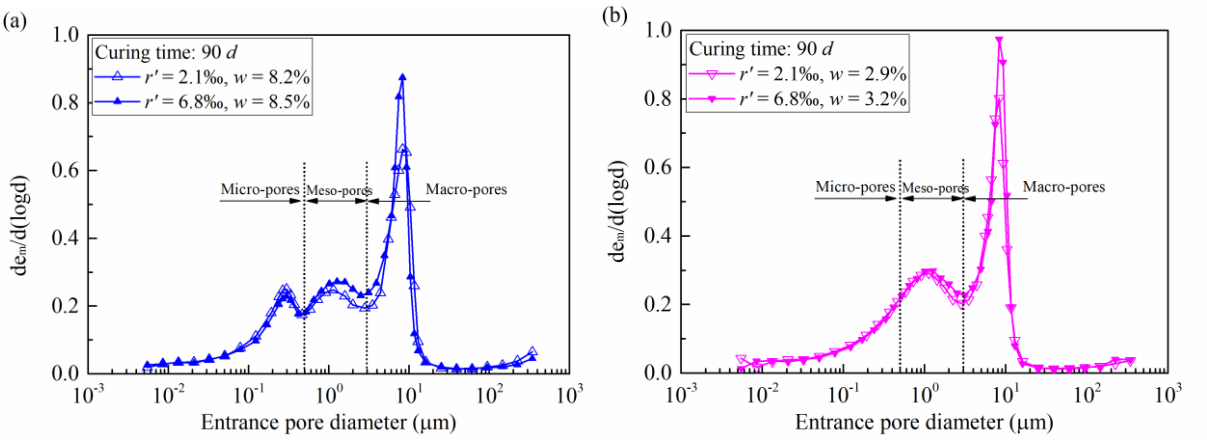


Fig. 8. Salinity effect on the pore size distribution for the lime-treated specimens after drying: (a) $w \approx 8\%$; (b) $w \approx 3\%$.

4. Discussions

4.1 Water retention capacity

Based on the PSD curves, the SWRCs of lime-treated specimens were deduced and presented in Figs. 9a and 9b for the specimens at 28-day and 90-day curing, respectively. The SWRCs of specimens at different water contents derived from the MIP tests are shown in dash/dot lines (MIP), and the curves of matric suction which was measured by filter paper method are presented in hollow signs (FP). It is observed that the SWRCs (MIP) of specimens at water content higher than 14% were characterized by two air entry values (AEVs) at suctions in the ranges of 30 ~ 40 kPa and 200 ~ 300 kPa, respectively. The corresponding entrance pore diameters at AEVs are shown in Fig. 5. It indicates that the two AEVs corresponded to the points at which the density function curves of macro-pores and meso-pores increased dramatically. With drying (w < 14%), only one AEV of macro-pores at low suction could be observed, while the AEV of meso-pores was not obvious due to the enlargement of meso-pores which exhibited a relatively lower increase in density function. It appears from Fig. 9b that the salinity effect on the SWRCs (MIP) was insignificant, whereas the specimens with higher soil salinity had relatively higher matric suctions measured by the filter paper method. Comparison between the SWRCs in Figs. 9a and 9b indicates that the curing time had insignificant effect on the SWRCs derived from the MIP results, which was different from the matric suction measured by filter paper method that increased noticeably as curing time increased from 28 days to 90 days (Fig. 3). Thus, a larger difference between the SWRCs from MIP tests and from filter paper measurements was observed for specimens at 90-day as compared to those at 28-

day curing. Wang et al. [9] and Sun and Cui [24] attributed this difference to the effect of volume change: the curve from MIP results did not include any effect of volume change, while that determined directly using filter paper method for suction measurement did. Indeed, as explained in the materials and methods section, each SWRC that consisted of several points in terms of matric suction versus water content, was derived from the MIP result of one specimen without considering the volume change. The points of specimens at different water contents (during drying) can be selected on the SWRCs (MIP) at the corresponding water contents and these points constituted the SWRCs in solid signs, namely SWRCs (MIP at each *w*). These SWRCs were considered involving the microstructure variations, as these points corresponded to different specimens during drying but not from one specimen. Nevertheless, these SWRCs (MIP at each *w*) were also different from the ones directly measured by the filter paper method.

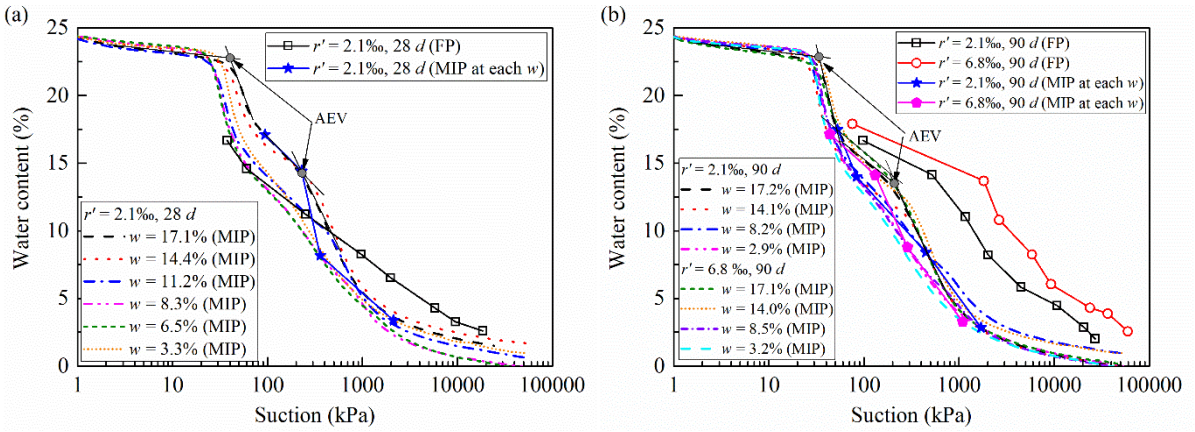


Fig. 9. Water retention curves in terms of matric suction from MIP tests and by filter paper method for suction measurement: (a) t = 28 days; (b) t = 90 days.

It appears from Eq. (3) that the value of the contact angle between the water-soil interface and the value of the surface tension of soil pore water might affect the matric suction deduced from the MIP results. The water-soil contact angle, θ_w, was widely taken as zero, assuming that the soil was a perfect hydrophilic material [45–48]. Li et al. [49] indicated that, when the contact angle of soil-water interface was taken as 70° and 50° for the wetting and drying process of loess, the SWRCs derived from MIP results agreed well with the measured ones. It was noting that the larger the contact angle, the lower the matric suction. As a result, a larger difference between the water retention curves derived from MIP results and filter paper measurement was obtained if a higher value of contact angle (> 0°) was taken. Sghaier et al. [50] and Leelamanie [51] indicated that the surface tension (T) and the contact angle (θ) increased with increasing salt concentration. However, the product of $T\cos\theta$ did not change appreciably with the salt

concentration. This suggested that the salinity effect on the surface tension and contact angle was not the main reason for the difference between the SWRCs derived from MIP results and filter paper measurement.

Romero et al. [5,29] indicated that the water retention property was dominated by the capillary force in low suction range, whereas the adsorptive force was the important factor in high suction range. The capillarity was highly related to the soil mineralogy and pore size distribution [52,53], while the adsorption was associated with soil mineralogy [52] and the specific surface area of the clayey fraction [54,55]. Tuller and Or [55] reported that the soil with higher specific surface area presented higher water adsorption capacity. The specific surface area of lime-treated soil was found to increase over curing time as the cementitious compounds were produced in the long-term reaction [56-58]. Muller [59] calculated the specific surface area of cementitious compounds (C-S-H) in cement paste using the results from Nuclear Magnetic Resonance (NMR) test. It was reported that the specific surface areas were 91 m^2/cm^3 for C-S-H gel pores and 175 m^2/cm^3 for interlayer spaces [59], which were higher than that of untreated soil. Ying et al. [60] performed XRD tests on the lime-treated soil (the same silt as in this study) and reported that the hydrated lime decreased from 2.1% at 1-day curing to 1.9% at 90-day curing, suggesting that the soil-lime reaction was developed and small amount of cementitious compounds was produced in this kind of silt. Thus, the difference between the water retention curves derived from MIP results and measured by contact filter paper method could be mainly attributed to the production of cementitious compounds which could improve the water adsorption capacity of soils. However, the cementitious compounds had slight effect on the PSD, and hence the SWRCs derived from MIP results. This was due to the low quantity of cementitious compounds which could only coat some surfaces of aggregates, leading to a slight decrease of micro-pores for this studied silt [38]. The longer the curing time, the more the production of cementitious compounds, thus the higher the matric suction measured. Therefore, the difference between the matric suctions from the filter paper measurement and derived from MIP results increased with increasing curing time from 28 days to 90 days. Moreover, at given curing time, this difference was larger for lime-treated soil with higher soil salinity (6.8‰ against 2.1‰). By contrast, it was found that the salinity had no or negligible effect on the matric suction of untreated soil, such as compacted kaolin and residual soil [22], fine sandy silt [41], and fine-grained soil [42]. This suggested that the increased matric suction of lime-treated soil with higher salinity might be due to the promotion of cementitious compounds production by salts.

Unlike the matric suction, the total suction did not exhibit significant changes over curing time, while it increased appreciably as the soil salinity increased (Figs. 3 and 4). Note that the total suction was determined through the measurement of relative humidity [17,21,22]. Leong et al. [22] measured the relative humidity of filter papers which were soaked with distilled water or sodium chloride (NaCl) solutions, and reported that the relative humidity decreased with the increase of salt concentration. This explains why the total suction which was composed of both matric and osmotic suctions increased significantly as soil salinity increased (Fig. 4). Al-Mukhtar et al. [61] stated that the electrical conductivity of soil-lime mixtures decreased during curing due to the cation exchanges and the consumption of Ca^{2+} and OH^- in the long-term pozzolanic reaction, suggesting that the osmotic suction of lime-treated specimens should decrease during curing. In addition, Hamidi et al. [62] reported that the precipitation of $CaCO_3$ and $Mg(OH)_2$ could occur in alkaline environment, consuming the Ca^{2+} and Mg^{2+} ions in soil pore water. Thus, at given water content, the insignificant effect of curing time on total suction can be attributed to the balance between the increased matric suction resulted from the production of cementitious compounds and the decreased osmotic suction due to the consumption of salts. Furthermore, upon drying, the matric suction increased, while the osmotic suction decreased due to the precipitation of salts, making the matric suction curves converge to the total suction curves at low water content (Fig. 3).

4.2 Microstructure

The MIP results showed that the PSD varied significantly during drying despite the similar global void ratio of specimens (Figs. 5 and 6). This can be attributed to the large amount of silt/sand grains (83%) constituting the skeleton of compacted specimens which can maintain the macro-pores and the global volume unchanged during drying. Indeed, Shi and Zhao [63] indicated that, for the soil with low clay fraction, the behaviour was dominant by the silt/sand grains. The association of silt/sand skeleton and clay film constituted soil aggregates. The macro-pores corresponded to the porosity between aggregates, and the micro-pores and meso-pores were related to the porosity of clays on the surface of these aggregates. The shrinkage of clay fraction led to an enlargement of the pore size between the aggregates on the one hand, and induced the development of some fissures in the clay fraction and at the interface between clay and silt/sand grains on the other hand [64–66]. Therefore, with the specimens being dried to 11.2% water content, the following phenomena were observed (Fig. 5): the peak pore entrance diameter between the micro-pores and meso-pores decreased as the nano-fissures (micro-pores) developed; a dominant peak of meso-pores started to emerge at around 1.5 μm

as some initial relative smaller meso-pores or micro-pores of the clay fraction became larger; the modal size of macro-pores enlarged and its frequency increased due to the enlargement of inter-aggregate pores which might be meso-pores initially. Correspondingly, the void ratio of micro-pores increased with the development of nano-fissures, while the void ratio of meso-pores decreased and that of macro-pores increased with decreasing water content to 11% due to the prevailing enlargement of meso-pores to macro-pores rather than the evolution of micro-pores to meso-pores (Fig. 6). Upon drying to 8% water content, the tri-modal pattern with populations of micro-pores, meso-pores and macro-pores was well formed, in which the micro-pores were mostly composed of drying-induced fissures. With further drying, the drying-induced fissures became larger and larger due to the continuous shrinkage of clay fraction, making the peak of micro-pores disappear gradually and the frequency of meso-pores increase (Fig. 5). Thus, the void ratio of micro-pores decreased, while the void ratio of meso-pores increased upon drying from 11.2% to 3.3% water content (Fig. 6).

When soil, lime and water were mixed together, the cation exchanges took place rapidly, making soil particles flocculate and forming coarser aggregates [1,3]. Bell [1,2] indicated that these modifications of soil particles induced by lime addition would largely reduce the plasticity and shrinkage of soil. Therefore, the lower frequency of drying-induced micro-pores and the smaller modal size of drying-induced meso-pores were observed on lime-treated specimens in comparison to the untreated specimens at water content of around 8% (Fig. 7a). The lime-treated specimens presented a higher frequency of macro-pores at 8% water content, which could be attributed to the flocculation of soil particles that produced more macro-pores in the lime-treated specimens. With further drying to 3% water content, the clay fraction in the untreated specimens suffered more significant shrinkage, giving rise to an increase of the frequency of macro-pores in the untreated specimens to the level of lime-treated specimens (Fig.7b). Nevertheless, the similar PSD curves were observed for the lime-treated specimens at different curing times (t = 28 days and 90 days). The insignificant effect of curing time on the drying-induced microstructure indicated that the production of cementitious compounds by pozzolanic reaction was limited due to the low reactivity of clay minerals (10.8% illite, 3.6% chlorite and 1.3% kaolinite), and inert phases of quartz (39%) and feldspar (9.5%) in the tested silt. It could not provide enough activated silica and alumina to interact with calcium to produce a significant amount of cementitious compounds. Indeed, Ying et al. [60] showed that the quantities of quartz, feldspar, illite, chlorite and kaolinite in the lime-treated soil (the same silt as in this study) after 90-day curing were rather similar to those of untreated soil, and no

significant cementitious compounds were identified through XRD analysis. Wang et al. [67] reported that the well-crystallized cementitious compounds could be identified in the lime-treated soil with large aggregates (D_{max} = 5 mm) after one year curing, while no XRD signal of cementitious compounds was detected on soil with smaller aggregates (D_{max} = 0.4 mm) due to the low quantity and low degree of crystallisation of cementitious compounds. Thus, it can be inferred that the low quantity of cementitious compounds produced in the tested silt might be in poorly-crystallized or amorphous phase that played a limited role in inhibition of clay shrinkage. This was consistent with the results obtained by Wang et al. [68], showing that the curing time effect was insignificant on the shrinkage behaviour of lime-treated soil. Ying et al. [33] indicated that, for the same silt with soil salinity of 6.32‰, some salts started to precipitate when the water content deceased to 8%, which might reduce the pore size. However, the slightly higher frequencies of macro-pores were obtained for the specimens with higher salinity (Fig. 8). This indicated that the enlargement of macro-pores due to the shrinkage of the diffuse double layer of clay minerals induced from salts prevailed over the decreased pore size due to the precipitated salts. However, this salinity effect was quite low owing to the low clay fraction (15.7%) in the tested silt [69].

5. Conclusions

The water retention property of lime-treated specimens was studied, with consideration of the curing time and salinity effects. The PSD variations in the lime-treated specimens along the SWRC were investigated by MIP tests. The difference between the SWRCs from filter paper measurement and from MIP tests was analyzed. On the basis of the results obtained, the following conclusions are drawn:

(1) The soil matric suction increased significantly during curing, due to the production of cementitious compounds which exhibited higher specific surface area, giving rise to an increase of water adsorption capacity of soils. Higher matric suctions were observed for the lime-treated specimens having higher salinity, suggesting that salts promoted the production of cementitious compounds. However, the curing time effect on the total suction was insignificant, which can be attributed to the balance between the increased matric suction and the decreased osmotic suction induced by the consumption of cations in the cation exchanges, pozzolanic reaction and salt precipitation.

(2) The SWRCs derived from MIP results of specimens at different water contents considering

the microstructure variations during drying were still different from those curves from direct measurement. This difference was mainly attributed to the production of cementitious compounds: the cementitious compounds with higher adsorption capacity did not contribute to the matric suctions derived from the MIP tests, but they significantly contributed to the matric suctions measured by the filter paper method.

(3) The PSD presented bi-modal characteristics for as-compacted specimens ($w \approx 17\%$) and air-dried specimens at water contents higher than 14%. Upon drying to 8% water content, a new peak pore developed gradually and the PSD changed to tri-modal pattern with three populations of micro-pores, meso-pores and macro-pores. With further drying to a water content of about 3%, the frequency of micro-pores decreased gradually, finally making the peak of the micro-pores disappear and the PSD recover to bi-modal characteristics. These variations of PSD could be attributed to the clay shrinkage of the clay fraction in the tested silt which was mainly constituted by silt/sand skeletons, leading to an enlargement of the meso-pore size and inducing the development of some fissures in the clay fraction and at the interface between clay and silt/sand grains.

(4) The curing time effect was found insignificant on the drying-induced microstructure changes, while the lime treatment effect was noticeable. Lime treatment resulted in rapid cation exchanges that made the soil particles flocculate and forming larger aggregates, inhibiting the clay shrinkage and attenuating the enlargement of pore size. The insignificant effect of curing time on the drying-induced microstructure could be attributed to the low reactivity of silty soil wilt lime, forming low quantity cementitious compounds that played a limited role in inhibiting clay shrinkage. The salinity effect on the drying-induced microstructure was visible but not significant, due to the low clay fraction in the tested silt.

It can be concluded that, for this lime-treated silt used for dike construction, drying resulted in shrinkage of clay fraction that altered the microstructure of soils, but did not induce the macro-cracks which could influence the sustainability of structures. The salts in synthetic seawater promoted the production of cementitious compounds which improved the water retention capacity of lime-treated soil and thus gave rise to higher resistance to climate changes, such as rainfall and water evaporation, etc. These results can be further used to interpret the hydro-mechanical behaviour of lime-treated silt.

CRediT authorship contribution statement

Zi Ying: Validation, Investigation, Writing - original draft. Yu-Jun Cui: Conceptualization, Methodology, Writing - review & editing. Nadia Benahmed: Investigation, Resources. Myriam Duc: Investigation.

Declaration of competing interest

The authors declare that they have no known competing financial interests or personal relationships that could have appeared to influence the work reported in this paper.

Acknowledgements

The authors would like to thank the China Scholarship Council (CSC). The supports provided by Ecole des Ponts ParisTech (ENPC) and INRAE are also greatly acknowledged.

References

[1] F.G. Bell, Lime stabilization of clay minerals and soils, Eng. Geol. 42 (1996) 223-237. https://doi.org/10.1016/0013-7952(96)00028-2.

[2] F.G. Bell, Lime stabilisation of clay soils, Bull. Int. Assoc. Eng. Geol. 39 (1989) 67-74. https://doi.org/10.1007/BF02592537.

[3] J. Locat, M.A. Berube, M. Choquette, Laboratory investigations on the lime stabilization of sensitive clays: shear strength development, Can. Geotech. J. 27 (1990) 294-304. https://doi.org/10.1139/t90-040.

[4] Y. Gao, Z. Li, D.A. Sun, H.H. Yu, A simple method for predicting the hydraulic properties of unsaturated soils with different void ratios, Soil Tillage Res. 209 (2021). 104913. https://doi.org/10.1016/j.still.2020.104913.

[5] E. Romero, A. Gens, A. Lloret, Water permeability, water retention and microstructure of unsaturated compacted Boom clay, Eng. Geol. 54 (1999) 117-127. https://doi.org/10.1016/S0013-7952(99)00067-8.

[6] W.S. Kim, R.H. Borden, Influence of soil type and stress state on predicting shear strength of unsaturated soils using the soil-water characteristic curve, Can. Geotech. J. 48 (2011) 1886-1900. https://doi.org/10.1139/T11-082.

[7] H. Tu, S.K. Vanapalli, Prediction of the variation of swelling pressure and one-dimensional heave of expansive soils with respect to suction using the soil-water retention curve as a tool, Can. Geotech. J. 53 (2016) 1213-1234. https://doi.org/ 10.1139/cgj-2015-0222.

[8] B. Le Runigo, O. Cuisinier, Y.J. Cui, V. Ferber, D. Deneele, Impact of initial state on the fabric and permeability of a lime-treated silt under long-term leaching, Can. Geotech. J. 46 (2009) 1243-1257. https://doi.org/10.1139/T09-061.

[9] Y.J. Wang, Y.J. Cui, A.M. Tang, C.S. Tang, N. Benahmed, Effects of aggregate size on water retention capacity and microstructure of lime-treated silty soil, Geotech. Lett. 5 (2015) 269-274. https://doi.org/10.1680/jgele.15.00127.

[10] G. Russo, G. Modoni, Fabric changes induced by lime addition on a compacted alluvial soil, Geotech. Lett. 3 (2013) 93-97. https://doi.org/10.1680/geolett.13.026.

[11] S.A.A. Khattab, L.K.I. Al-Taie, Soil-water characteristic curves (SWCC) for lime treated expansive doil from Mosul city, Unsaturated Soils (2006) 1671-1682. https://doi.org/10.1061/40802(189)140.

[12] D. V. Tedesco, G. Russo, Time dependency of the water retention properties of a lime stabilised compacted soil, Unsaturated Soils: Advances in Geo-Engineering. Taylor & Francis Group, London (2008) 277-282. https://doi.org/10.1201/9780203884430.ch33.

[13] X. Bian, L.L. Zeng, X.Z. Li, X.S. Shi, S.M. Zhou, F.Q. Li, Fabric changes induced by super-absorbent polymer on cement–lime stabilized excavated clayey soil, J. Rock Mech. Geotech. Eng. (2021). https://doi.org/10.1016/j.jrmge.2021.03.006.

[14] H.N. Ramesh, M.S. Mohan, P. V. Sivapullaiah, Improvement of strength of fly ash with lime and sodium salts, Gr. Improv. 3 (1999) 163-167. https://doi.org/10.1680/gi. 1999.030403.

[15] R.B. Saldanha, H.C.S. Filho, J.L.D. Ribeiro, N.C. Consoli, Modelling the influence of density , curing time , amounts of lime and sodium chloride on the durability of compacted geopolymers monolithic walls, Constr. Build. Mater. 136 (2017) 65-72. https://doi.org/10.1016/j.conbuildmat.2017.01.023.

[16] H.F. Xing, X.M. Yang, C. Xu, G.B Ye, Strength characteristics and mechanisms of salt-rich soil-cement, Eng. Geol. 103 (2009) 33-38. https://doi.org/10.1016/j.enggeo.2008. 07.011.

[17] E.C. Leong, S. Tripathy, H. Rahardjo, Total suction measurement of unsaturated soils with a device using the chilled-mirror dew-point technique, Géotechnique. 53 (2003) 173-182. https://doi.org/10.1680/geot.53.2.173.37271.

[18] T. Thyagaraj, U. Salini, Effect of pore fluid osmotic suction on matric and total suctions of compacted clay, Géotechnique. 65 (2015) 952-960. https://doi.org/10.1680/jgeot. 14.P.210.

[19] ASTM D5298-16. Standard Test Method for Measurement of Soil Potential (Suction) Using Filter Paper. ASTM International, West Conshohocken, PA. 2016.

[20] S. Sreedeep, D.N. Singh, A study to investigate the influence of soil properties on suction, J. Test. Eval. 33 (2005) 61-66. https://doi.org/10.1520/jte11981.

[21] D.G. Fredlund, H. Rahardjo, Soil mechanics for unsaturated soils, John Wiley & Sons, New York, 1993.

[22] E.C. Leong, S. Widiastuti, C.C. Lee, H. Rahardjo, Accuracy of suction measurement, Géotechnique. 57 (2007) 547-556. https://doi.org/10.1680/geot.2007.57.6.547.

[23] J.A. Muñoz-Castelblanco, J.M. Pereira, P. Delage, Y.J. Cui, The water retention properties of a natural unsaturated loess from northern France, Géotechnique. 62 (2012) 95-106. https://doi.org/10.1680/geot.9.P.084.

[24] W.J. Sun, Y.J. Cui, Determining the soil-water retention curve using mercury intrusion porosimetry test in consideration of soil volume change, J. Rock Mech. Geotech. Eng. 12 (2020) 1070-1079. https://doi.org/10.1016/j.jrmge.2019.12.022.

[25] P.H. Simms, E.K. Yanful, Measurement and estimation of pore shrinkage and pore distribution in a clayey till during soil-water characteristic curve tests, Can. Geotech. J. 38 (2001) 741-754. https://doi.org/10.1139/cgj-38-4-741.

[26] P.H. Simms, E.K. Yanful, Predicting soil-water characteristic curves of compacted plastic soils from measured pore-size distributions, Géotechnique. 52 (2002) 269-278. https://doi.org/10.1680/geot.2002.52.4.269.

[27] O. Cuisinier, L. Laloui, Fabric evolution during hydromechanical loading of a compacted silt, Int. J. Numer. Anal. Methods Geomech. 28 (2004) 483-499. https://doi.org/10.1002/nag.348.

[28] A. Koliji, L. Laloui, O. Cusinier, L. Vulliet, Suction induced effects on the fabric of a structured soil, Transp. Porous Media. 64 (2006) 261-278. https://doi.org/10.1007/s11242-005-3656-3.

[29] E. Romero, G. Della Vecchia, C. Jommi, An insight into the water retention properties of compacted clayey soils, Géotechnique. 61 (2011) 313-328. https://doi.org/10.1680/geot.2011.61.4.313.

[30] G. Stoltz, O. Cuisinier, F. Masrouri, Multi-scale analysis of the swelling and shrinkage of a lime-treated expansive clayey soil, Appl. Clay Sci. 61 (2012) 44-51. https://doi.org/10.1016/j.clay.2012.04.001.

[31] M. Nabil, A. Mustapha, S. Rios, Long term evaluation of wetting-drying cycles for compacted soils treated with Lime, In Conference of the Arabian Journal of Geosciences. (2018) 277-281. https://doi.org/10.1007/978-3-030-01665-4.

[32] N. Poncelet, B. François, Desiccation crack in lime-treated silty clay: Experimental evaluation and constitutive interpretation, E3S Web Conf. 92 (2019) 1-6. https://doi.org/10.1051/e3sconf/20199211002.

[33] Z. Ying, M. Duc, Y.J. Cui, N. Benahmed, Salinity assessment for salted soil considering both dissolved and precipitated salts, Geotech. Test. J. 44 (2021) 130-147. https://doi.org/10.1520/GTJ20190301.

[34] French standard AFNOR NF P 18-837, Standard for special products for hydraulic concrete construction-Hydraulic binder based needling and/or sealing products-Testing of resistance against seawater and/or water with high sulphate contents. Association Francaise de Normalisation. (1993).

[35] P. Delage, G. Lefebvre, Study of the structure of a sensitive Champlain clay and of its evolution during consolidation, Can. Geotech. J. 21 (1984) 21-35. https://doi.org/10.1139/t84-003.

[36] C.H. Juang, R.D. Holtz, A probabilistic permeability model and the pore size density function, Int. J. Numer. Anal. Methods Geomech. 10 (1986) 543-553. https://doi.org/10.1002/nag.1610100506.

[37] E. Romero, Thermo-hydro-mechanical behaviour of unsaturated boom clay: an experimental study. PhD Thesis, Universidad Politécnica de Catalunya, Barcelona, Spain. (1999).

[38] Z. Ying, Y.J. Cui, N. Benahmed, M. Duc, Changes of microstructure and water retention property of a lime-treated saline soil during curing, Acta Geotech. (2021). https://doi.org/10.1007/s11440-021-01218-5.

[39] S. Sreedeep, D.N. Singh, Methodology for determination of osmotic suction of soils,

Geotech. Geol. Eng. 24 (2006) 1469-1479. https://doi.org/10.1007/s10706-005-1882-7.

[40] Y.F. Arifin, T. Schanz, Osmotic suction of highly plastic clays, Acta Geotech. 4 (2009) 177-191. https://doi.org/10.1007/s11440-009-0097-0.

[41] D.J. Miller, J.D. Nelson, Osmotic suction in unsaturated soil mechanics, in: Unsaturated Soils 2006, American Society of Civil Engineers, Reston, VA, 2006: pp. 1382-1393. https://doi.org/10.1061/40802(189)114.

[42] S. Sreedeep, D.N. Singh, Critical review of the methodologies employed for soil suction measurement, Int. J. Geomech. 11 (2011) 99-104. https://doi.org/10.1061/(asce)gm.1943-5622.0000022.

[43] Z. Ying, Y.J. Cui, N. Benahmed, M. Duc, Salinity effect on the compaction behaviour, matric suction, stiffness and microstructure of a silty soil, J. Rock Mech. Geotech. Eng. (2021). https://doi.org/10.1016/j.jrmge.2021.01.002.

[44] A.W.L. Wan, M.N. Gray, J. Graham, On the relations of suction , moisture content and soil structure in compacted clays, Proc. 1st Int. Conf. on Unsaturated Soils, Paris. Vol. 1. Balkema/Presses des Ponts et Chaussées. (1995).

[45] K.K. Aung, H. Rahardjo, E.C. Leong, D.G. Toll, Relationship between porosimetry measurement and soil-water characteristic curve for an unsaturated residual soil, Geotech. Geol. Eng. 19 (2001) 401-416. https://doi.org/10.1023/A:1013125600962.

[46] X. Li, L.M. Zhang, Characterization of dual-structure pore-size distribution of soil, Can. Geotech. J. 46 (2009) 129-141. https://doi.org/10.1139/T08-110.

[47] Y.J. Wang, Y.J. Cui, A.M. Tang, C.S. Tang, N. Benahmed, Changes in thermal conductivity, suction and microstructure of a compacted lime-treated silty soil during curing, Eng. Geol. 202 (2016) 114-121. https://doi.org/10.1016/j.enggeo.2016.01.008.

[48] G. Niu, D.A. Sun, L.T. Shao, L.F. Zeng, The water retention behaviours and pore size distributions of undisturbed and remoulded complete-intense weathering mudstone, Eur. J. Environ. Civ. Eng. (2019) 1233-1250. https://doi.org/10.1080/19648189.2019.1572544.

[49] H. Li, T.L. Li, P. Li, Y.G. Zhang, Prediction of loess soil-water characteristic curve by mercury intrusion porosimetry, J. Mt. Sci. 17 (2020) 2203-2213. https://doi.org/10.1007/s11629-019-5929-2.

[50] N. Sghaier, M. Prat, S. Ben Nasrallah, On the influence of sodium chloride concentration on equilibrium contact angle, Chem. Eng. J. 122 (2006) 47-53. https://doi.org/10.1016/j.cej.2006.02.017.

[51] D.A.L. Leelamanie, J. Karube, Soil-water contact angle as affected by the aqueous electrolyte concentration, Soil Sci. Plant Nutr. 59 (2013) 501-508. https://doi.org/10.1080/00380768.2013.809601.

[52] N. Lu, M. Khorshidi, Mechanisms for Soil-Water Retention and Hysteresis at High Suction Range, J. Geotech. Geoenviron. Eng. 141 (2015) 04015032. https://doi.org/10.1061/(asce)gt.1943-5606.0001325.

[53] C.W.W. Ng, H. Sadeghi, S.K.B. Hossen, C.F. Chiu, E.E. Alonso, Water retention and volumetric characteristics of intact and re-compacted loess, Can. Geotech. J. 53 (2016) 1258-1269. https://doi.org/doi.org/10.1139/cgj-2015-0364.

[54] E. Romero, J. Vaunat, Retention curves of deformable clays, Experimental Evidence and Theoretical Approaches in Unsaturated Soils. (2000) 91-106.

[55] M. Tuller, D. Or, Water films and scaling of soil characteristic curves at low water contents, Water Resour. Res. 41 (2005) 1-6. https://doi.org/10.1029/2005WR004142.

[56] E. Vitale, D. Deneele, M. Paris, G. Russo, Multi-scale analysis and time evolution of pozzolanic activity of lime treated clays, Appl. Clay Sci. 141 (2017) 36-45. https://doi.org/10.1016/j.clay.2017.02.013.

[57] L.K. Sharma, N.N. Sirdesai, K.M. Sharma, T.N. Singh, Experimental study to examine the independent roles of lime and cement on the stabilization of a mountain soil: A comparative study, Appl. Clay Sci. 152 (2018) 183-195. https://doi.org/10.1016/j.clay.2017.11.012.

[58] W.P. Halperin, J.Y. Jehng, Y.. Song, Application of spin-spin relaxation to measurement of surface area and pore size distributions in a hydrating cement paste, Magn. Reson. Imaging. 12 (1994) 169-173. https://doi.org/doi.org/10.1016/0730-725X(94)91509-1.

[59] A.C.A. Muller, Characterization of porosity & C-S-H in cement pastes by 1H NMR, PhD Thesis, École Polytechnique Fédérale de Lausanne, Lausanne, Suisse. (2014).

[60] Z. Ying, Y.J. Cui, N. Benahmed, M. Duc, Changes in mineralogy and microstructure of a lime-treated silty soil during curing time, 4th European Conference on Unsaturated soils. Lisbon. (2020). https://doi.org/10.1051/e3sconf/202019503044.

[61] M. Al-Mukhtar, A. Lasledj, J.F. Alcover, Behaviour and mineralogy changes in lime-treated expansive soil at 20°C, Appl. Clay Sci. 50 (2010) 191-198. https://doi.org/10.1016/j.clay.2010.07.023.

[62] R. Hamidi, D. Kahforoushan, E. Fatehifar, M. Arehjani, S. Farmanbordar, Simultaneous removal of Ca and Mg salts using chemical precipitation with lime, The 7th International Chemical Engineering Congress & Exhibition. Kish, Iran, 21-24 November, (2011).

[63] X.S. Shi, J.D. Zhao, Practical estimation of compression behavior of clayey/silty sands using equivalent void-ratio concept, J. Geotech. Geoenviron. Eng. 146 (2020) 04020046. https://doi.org/10.1061/(asce)gt.1943-5606.0002267.

[64] C.S. Tang, B. Shi, C. Liu, W. W.B. Suo, L. Gao, Experimental characterization of shrinkage and desiccation cracking in thin clay layer, Appl. Clay Sci. 52 (2011) 69-77. https://doi.org/10.1016/j.clay.2011.01.032.

[65] W.J. Sun, Y.J. Cui, Investigating the microstructure changes for silty soil during drying, Géotechnique. 68 (2018) 370-373. https://doi.org/10.1680/jgeot.16.P.165.

[66] Z. Ying, Y. Cui, N. Benahmed, M. Duc, Drying effect on the microstructure of compacted salted silt, Géotechnique. (2021) Accepted for publication.

[67] Y.J. Wang, M. Duc, Y.J. Cui, A.M. Tang, N. Benahmed, W.J. Sun, W.M. Ye, Aggregate size effect on the development of cementitious compounds in a lime-treated soil during curing, Appl. Clay Sci. 136 (2017) 58-66. https://doi.org/10.1016/j.clay.2016.11.003.

[68] Y.J. Wang, Y.J. Cui, A.M. Tang, N. Benahmed, M. Duc, W.J. Sun, Shrinkage behaviour of a compacted lime-treated clay, Geotech. Lett. 10 (2020) 174-178. https://doi.org/10.1680/jgele.19.00006.

[69] Z. Ying, Y.J. Cui, M. Duc, N. Benahmed, H. Bessaies-Bey, B. Chen, Salinity effect on the liquid limit of soils, Acta Geotech. 16 (2021) 1101-1111. https://doi.org/10.1007/s11440-020-01092